Article **Journal Renewable Energy**
December, 2023 Vol.7 No.19 19-27

Design considerations for the dimensioning of parabolic trough solar thermal plants

Consideraciones de diseño para el dimensionamiento de plantas solares térmicas de concentrador parabólico

LIZÁRRAGA-MORAZÁN, Juan Ramón† & PICÓN-NUÑEZ, Martin

Department of Chemical Engineering, Division of Natural and Exact Sciences, University of Guanajuato, Mexico.

ID 1er Author: *Juan Ramón, Lizárraga-Morazán* / **ORC ID**: 0000-0002-7733-5621, **CVU CONAHCYT ID**: 83138

ID 1st Co-author: *Martin, Picón-Nuñez* / **ORC ID**: 0000-0002-0793-192X, **CVU CONAHCYT ID** 12408

DOI: 10.35429/JRE.2023.19.7.19.27 Received July 30, 2023; Accepted October 30, 2023

Abstract

Solar heaters of the parabolic trough type, PTC, are a proved technology that has a wide diversity of industrial applications. The prediction of the thermal conditions in these devices plays a fundamental role in the development and design of thermal plants capable of meeting the heat load requirements. To this end highly complex thermal models have been derived which are difficult to solve and implement. This work puts forward a PTC transient thermal model which was validated using experimental data and compared against other theoretical models existing in the open literature. Along with this model, a novel sequential solution procedure is proposed with which a better follow up of variable outputs is obtained. A parametric analysis was carried out of for the main design variables using the Present Value of the Life Cycle Energy Savings (PVLCES) and Total Integrated Heat (TIH) using daily typical data in the winter and summer seasons for the city of Guanajuato. Due to its transient nature, the model can be implemented in research where optimisation tools are required such as Deep Learning, Machine Learning and Control, which are basic in the dimensioning of thermal solar plants.

Parabolic trough solar collectors, Thermal design, Thermal performance, Solar field sizing, Solar thermal energy

Resumen

Los calentadores solares tipo parabólico, PTC, son una tecnología ya probada con una gran diversidad de aplicaciones industriales. La predicción de las condiciones térmicas de estos equipos juega un papel fundamental para el desarrollo y diseño de plantas termosolares capaces de cumplir con los requerimientos y cargas térmicas. Con este fin se han desarrollado modelos térmicos altamente complejos que presentan dificultades para su implementación y solución. En este trabajo se propone un modelo térmico para la tecnología PTC en estado transiente unidimensional, que fue validado con datos experimentales y comparado con otros modelos existentes en literatura. Con el modelo, se propone un procedimiento novedoso de solución de tipo secuencial, con el que se tiene un mejor seguimiento de los resultados de las variables. Se realizó un análisis paramétrico de las principales variables de diseño del equipo empleando como indicadores el Valor Presente del Análisis del Ciclo de Vida (PVLCES por sus siglas en inglés) y el Calor Total Integrado (TIH por sus siglas en inglés) con datos diarios típicos estacionales de invierno y verano para la ciudad de Guanajuato. Dada su naturaleza transiente, el modelo puede ser implementado para el desarrollo de investigaciones que requieran el empleo de las herramientas de optimización, Deep Learning, Machine Learning y de Control, que actualmente son básicas en el dimensionamiento de estas redes termosolares.

Colectores solares de tipo parabólico, Diseño térmico, Desempeño térmico, Dimensionamiento de campos solares, Energía solar térmica

Citation: LIZÁRRAGA MORAZÁN, Juan Ramón & PICÓN-NUÑEZ, Martin. Design considerations for the dimensioning of parabolic trough solar thermal plants. Journal Renewable Energy. 2023. 7-19: 19-27

* Author Correspondence (e-mail: lizarragamorazan@hotmail.com)
† Researcher contributing as first author.

Introduction

The constant growth of industrial activity is a core issue for counties to achieve its economical sustainability. Such development goes hand in hand with energy consumption. According to IEA (International Energy Agency), the share of the industrial sector is 32 % of the total energy consumption [I]. International agreements and the 2030 UN agenda foster the use of clean energy to curb environmental pollution. The economic reactivation after the Covid-19 pandemic and the response to the global energy crisis have driven investment in clean energy, reaching 1.7 trillion USD over the first half of 2023; with fossil energy investment of only about 0.9 trillion USD [II]. It is foreseen that the substitution of fossil fuel by clean energy will be achieved by 2050, although it depends on the implementation and the support of suitable local and international policies [III].

Solar energy is a limitless and clear energy source that is harnessed employing technologies referred to as SHIP (solar heat for industrial processes) that include CSP (concentrated solar power), PV (photovoltaic), solar Chemistry, solar desalination, and solar cooling amidst others [IV], [V]. The total installed accumulated capacity in operation by the end of 2022 was 542 GW_{th}, which corresponds to 774 million square meters of solar collectors that represent an increment of 19 GW_{th} or 27.1 million surface area [VI]. Most of these plants employ solar heaters of the PTC type (parabolic trough collectors) [VII], as in 2022, 90 % of these solar plants used this technology [VIII]. These devices can be applied in a temperature range between 50 and 400 °C [IX].

Given the great diversity and wide application spectrum of the PTC technology, the development of theoretical models to predict its performance is paramount. Diverse models have been published in the open literature, some of them employ commercial simulation tools for its solution, while other models have been solved using other type of codes. Zima et al. [X] developed a one-dimensional model to simulate the transient performance of a PTC with a U tube for the residential sector. The model was successfully compared with a three-dimensional model coded in Ansys Fluent CFD and with experimental data.

Behar *et al*. [XI], developed a steady state model and its results were compared with experimental data achieving a close fit with an uncertainty of 0.64 %. Ferchichi *et al*. [XII] proposed a discretised model for the prediction of phase change and heat transfer for a steam generation system (DSG - Direct Steam Generation) that operates with PTC. The code was written in C^{++}. Xu et. al. [VII], established and validated a one-dimensional transient model and carried out a parametric study considering the inlet temperature of the working fluid (HTF), ambient conditions and optical efficiency. Mouaky *et al*. [XIII], simulated a four-module PTC developed by Soltigua using the Ebsilon® Professional platform. The model was validated using operating data under clear sky conditions with a maximum deviation of 4.8 %. Krishna *et al*. [XIV], employed the TRNSYS platform to simulate a phase change domestic solar PTC heater to predict the availability of hot water during the peak demand of hot water in Mangalore, India. They concluded that the system could meet the thermal duty.

From the previous review it can be observed that the steady state and transient models reproduce in a satisfactory manner the performance of PTC devices. The transient model, however, bears greater advantages in terms of control despite the highest computational needs. Additionally, all these models have been validated using fix ambient conditions within three and four consecutive days. Such experimentation does not cover the totality of seasonal and daily conditions. In this work a new one-dimensional transient model is proposed and is validated against experimental data reported in the open literature. The model was analysed under diverse seasonal and daily ambient conditions. The economic viability of a solar thermal plant using PTC technology is assessed using the pumping costs and the net present value of the life cycle energy savings.

Methodology

The transient state energy equation and the rest of the expressions that make up the model based on the representation of the phenomenon schematised in Figure 1 are presented below:

$$\frac{dQ}{dt} = F_R[G_{BH}\eta_0 A_a - A_r U_L(T_i - T_a)] \quad (1)$$

$$\frac{A_a}{A_r} = \frac{1}{\pi sin(\theta_m)} = C \quad (2)$$

ISSN 2523-2881

$$U_L = \left[\frac{A_r}{(h_{fi} + h_{r,c-a})A_a} + \frac{1}{h_{r,p-c}}\right]^{-1} \quad (3)$$

$$h_{r,c-a} = 4\sigma\varepsilon_g T_g^3 \quad (4)$$

$$h_{r,p-c} = \frac{\sigma(T_p - T_g)(T_p^2 + T_g^2)}{\left(\frac{1}{\varepsilon_p}\right) + \left(\frac{1}{\varepsilon_c} - 1\right)\left(\frac{A_r}{A_a}\right)} \quad (5)$$

$$F_r = \frac{\dot{m}c_p}{A_r U_L}\left[1 - exp\left(-\frac{U_L F' A_r}{\dot{m}c_p}\right)\right] \quad (6)$$

$$F' = \frac{\frac{1}{U_L}}{\frac{1}{U_L} + \frac{D_0}{h_w D_i} + \left[\frac{D_0}{2k_r} ln\left(\frac{D_0}{D_i}\right)\right]} \quad (7)$$

$$D_0 = 2r_r sin(\theta_m) \quad (8)$$

$$r_r = \frac{2f}{1 + cos(\varphi_r)} \quad (9)$$

$$Q = \dot{m}c_p(T_0 - T_i) \quad (10)$$

$$A_g(h_{r,c-a} + h_{c,c-a})(T_g - T_a) - A_r h_{r,p-c}(T_p - T_g) = 0 \quad (11)$$

$$T_p = \frac{Q}{h_w \pi D_i L} + T_f \quad (12)$$

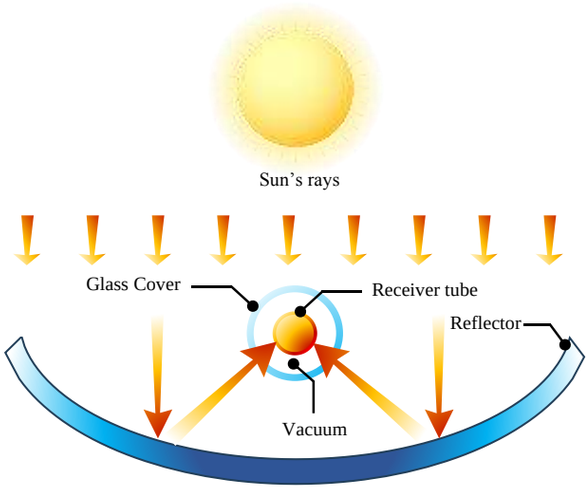

Figure 1 Schematic representation of a Parabolic Through Solar Collector

Where G_{BH} is the direct solar radiation, A_a and A_r are the aperture area and the receiver area, respectively; Q is the heat gained by the heat transfer fluid (HTF); F_R removal factor; U_L global coefficient of losses; $\theta_m$is the mean acceptance angle; T_i , T_0 and T_a are the inlet and outlet temperatures of the receiving tube, and the ambient temperature, respectively; F' the thermal efficiency factor; D_i and D_0 are the internal and external diameter of the receiving tube; $\dot{m}$ and $c_p$are the mass flow and heat capacity of the HTF; C is the solar concentration factor; f is the parabola focal length; h_w, $h_{r,c-a}$ and $h_{r,p-c}$ are the convective heat transfer coefficient of the HTF, the radiation from the glass cover to the environment, and the radiation from the receiver tube to the glass cover, respectively; r_r is the radius of the tube; and φ_r is the diffuse angle.

The transient energy balance is numerically solved using Butcher's fifth order Runge-Kutta methodology [XV]. The irradiance data used was obtained from the McClear model validated with experimental data. McClear is a clear-sky radiation model developed in the Copernicus program by the ECMWF - European Centre for Medium-Range Weather Forecasts -, which conducts non-profit research [XVI]. The environmental data of irradiance, ambient temperature, daily and seasonal wind speed was collected for the city of Guanajuato (21.0190° N, 101.2574° W) at the facilities of the University of Guanajuato, Mexico. The incidence angle of the solar rays (θ_B), and the optical efficiency, η_0 are calculated from the following expressions:

$$\eta_0 = \rho_0 \tau_g \alpha_r \gamma \left[\left(1 - A_f tan(\theta_B) cos(\theta_B)\right)\right] \quad (13)$$

$$\cos(\theta_B) = \sqrt{1 - cos^2(\delta) sin^2(h)} \quad (14)$$

Where δ is the declination angle, h is the hour angle, α_r is the receiver absorbance, τ_g is the transmittance of the tube envelope, and A_f is a geometric factor. A model code was written using the Matlab platform. Unlike the other models reported in the literature in which the equation system that makes up the model is solved simultaneously by means of an algorithm already implemented as a module, the new solution procedure is characterized by its sequential approach, which facilitates the follow-up of variables and allows control over the solution due to their high non-linearity that leads to more than one possible solution.

ISSN 2523-2881

It includes the determination of the outlet temperature and that of the glass envelope by means of the false rule method [XV], which ensures finding the correct value. Figure 2 shows the flow diagram for the solution of the model.

To ensure that the design is economically feasible, the proposed model was complemented with the *Present value of the Life Cycle Energy Savings* (PVLCES). Life Cycle Energy Savings Analysis is the difference between the life cycle cost of a system that provides an energy demand using conventional fossil energy and the life cycle cost of a solar system that provides the same energy load. The life cycle savings determine the net present value of the gain of the solar system compared to that of the conventional system [IX].

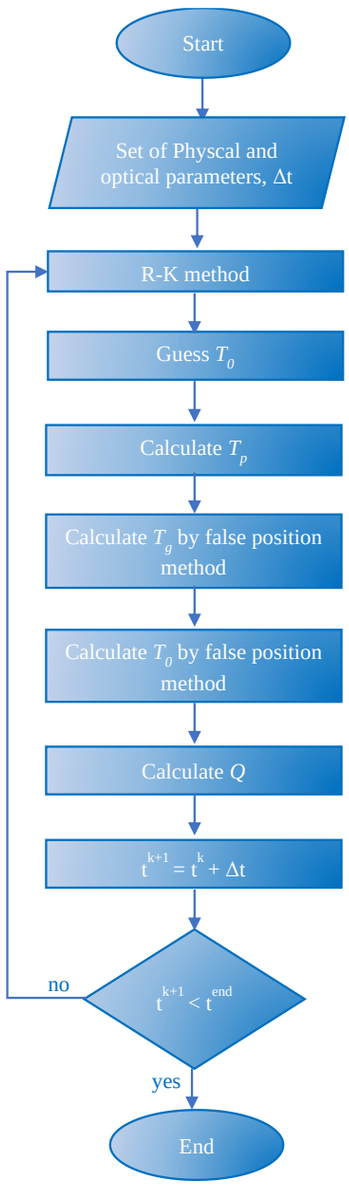

Figure 2 Flow diagram for the solution of the PTC model

The methodology reported in [XVII] was used to calculate the life cycle savings. The lifetime of the considered equipment was 25 years. Equation (15) is a general expression of economic analysis in which each of the components is calculated considering the time value of money.

$$Solar\ system\ savings = Fuel\ savings - loan\ payment - Maintaenance\ costs - insurance\ payment - Auxiliary\ energy\ costs - taxes \quad (15)$$

where,

$$Fuel\ savings = Solar\ fraction \cdot cost\ of\ fuel \cdot heat\ load \quad (16)$$

The system has a higher economic feasibility as the value of the life cycle savings increases. This analysis includes the thermal efficiency of the solar system which is represented in the economic savings of fossil fuel. On the other hand, it contemplates investment expenses, loans, taxes, operating costs (including pumping), fixed and variable maintenance in a defined time horizon.

Results

The validation of the model is done by the comparison with the experimental data reported by the Sandia National Laboratory (SNL) [XVII]. The experimental data was obtained for collectors operating with vacuum in the space of the glass envelope. The experimental tests were applied to the LS-2 solar collector installed on the AZTRAK platform at the SNL facilities. The dimensions of the system are presented in Table 1. These tests were carried out in a temperature range between 100 °C to 400 °C using water and Syltherm 800 as working fluids.

The comparative variation of the efficiency and thermal losses of the collector are presented in Figures 3 and 4. It is observed that the thermal efficiency decreases with respect to the temperature, contrary to the behaviour of the thermal losses. With the proposed model, a root mean square error (RMSE) of 1.39 °C is obtained in the prediction of the outlet temperature, with an average error of 0.24 %. For comparison purposes, Table 2 shows the mean square error of the efficiency and thermal losses calculated with other theoretical models reported in the literature.

ISSN 2523-2881

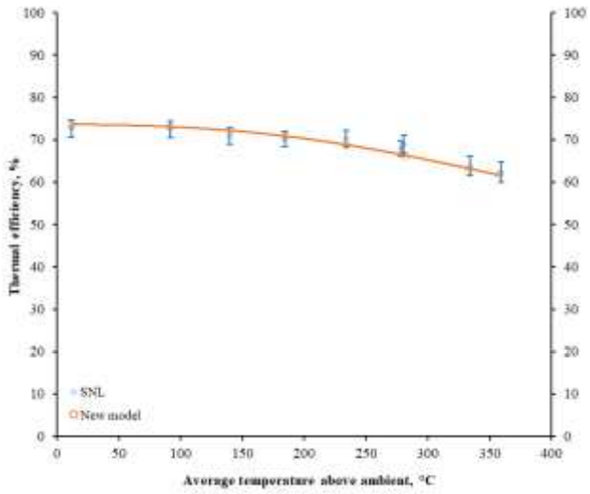

Figure 3 Comparison of the thermal efficiency calculated with the new model and the experimental data reported by SNL.

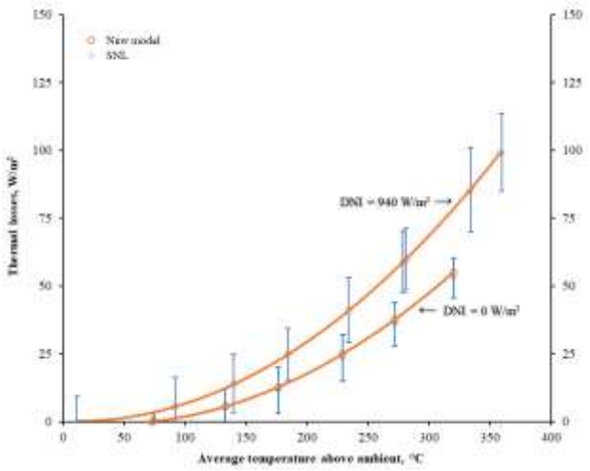

Figure 4 Comparison of thermal losses calculated with the new model and those reported by SNL.

Dimensions	Value, m
Aperture width	5
Length	7.8
Focal distance	1.84
Receiver tube inner diameter	0.066
Receiver tube outer diameter	0.07
Glass cover inner diameter	0.109
Glass cover outer diameter	0.115

Table 1 Dimensions of PTC LS-2 tested in SNL.

An analysis of the temperature and useful heat for commercial PTC dimensions [XVIII] was carried out assuming average winter and summer days of the city of Guanajuato, Mexico. The HTF used is Syltherm 800.

Model	η_t (%)	Thermal losses (W/m^2)
New model	1.019	0.368
Yilmaz and Söylemez [XIX]	0.766	4.638
Padilla *et al*. [XX]	1.012	10.255
NREL [XX1]	1.382	14.718
García-Valladares and Velázquez [XXII]	1.433	--

Table 2 RMSE comparison with some reported models.

Figures 5 and 6 show temperature and heat load profiles assuming working fluid inlet temperature in the range of 30 to 110 °C.

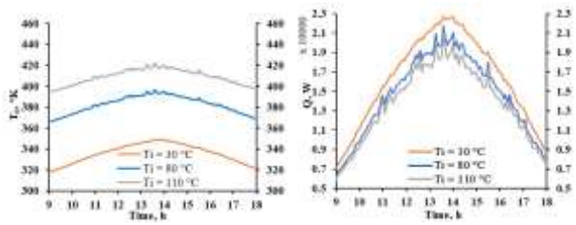

Figure 5 Temperature and heat load profile for a range of inlet temperatures (T_i) and mass flow rate $\dot{m}$ = 0.30 kg/s for a typical day in summer

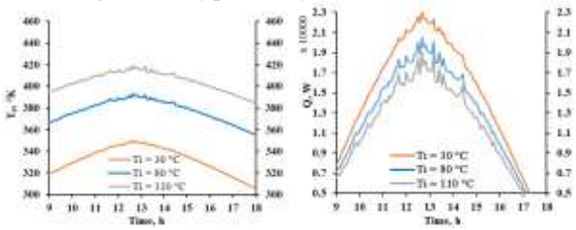

Figure 6 Temperature and heat load profile for a range of inlet temperatures (T_i) and mass flow rate $\dot{m}$ = 0.30 kg/s for a typical day in winter

Figure 7 illustrates the effect of the working fluid inlet temperature on the integrated heat of the PTC device.

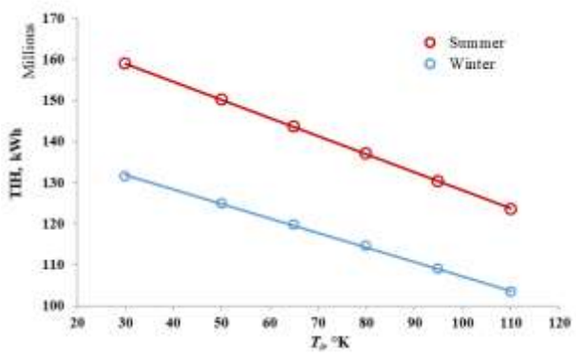

Figure 7 Effect of inlet temperature, T_i, on the total integrated heat for typical days in summer and winter and mass flow rate $\dot{m}$ = 0.30 kg/s

ISSN 2523-2881

Figure 7 shows the reduction of the integrated useful heat with the increment of inlet temperature of the HTF. The data shows a linear profile. The model provides the temperature and integrated heat load for any set of ambient conditions.

The variation of the mass flow rate between 0.3 and 0.6 kg/s and its effect on outlet temperature and heat load is depicted in Figures 8 and 9 for typical days in summer and winter. In these calculations, the inlet temperature was kept at 80 °C.

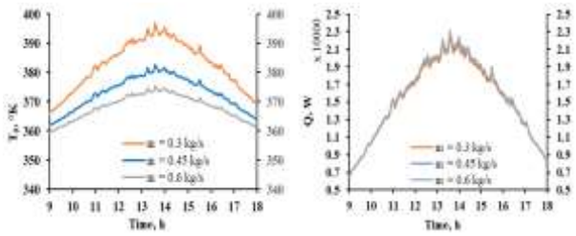

Figure 8 Effect of mass flow, $\dot{m}$, on outlet temperature, T_0, and thermal load, Q. T_i= 80 °C. Typical day of summer

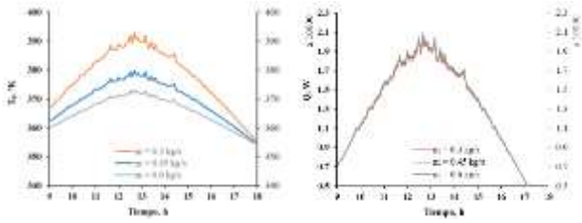

Figure 9 Temperature and heat load profile for different mass flow rates and T_i = 80 °C. Typical day in Winter

Figure 10 shows the effect of the mass flow rate on the integrated heat. A parametric study was also performed to analyse the effect of the design variables on the PTC using the *Present value of the Life Cycle Energy Savings* (PVLCES) and the integrated useful heat (TIH). This indicator is the integration of the instantaneous heat gained by the HTF between 9:00 and 18: 00 h:

$$TIH = Total\ Integrated\ Heat = \int_{t=9\ h}^{t=18\ h} q_t \qquad (17)$$

Where q_t is the instantaneous heat gained by the HTF.

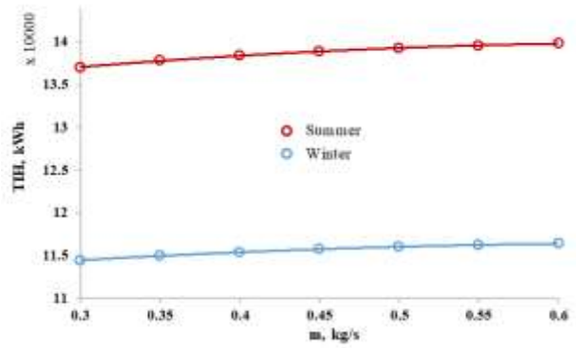

Figure 10 Effect of mass flow rate on the total integrated useful heat for typical days in summer and winter and T_i = 80 °C

The parametric study is carried out considering the following design variables: length, collector aperture, focal length, inner diameter of the receiver tube and inner diameter of the transparent glass cover (Table 3). Additionally, four different heat transfer fluids were analysed: Dowtherm A, Syltherm 800, Therminol VP-1, and pressurised water. The range of variation of each of the variables was taken from the data reported in the open literature for commercial collectors [XXIII].

Dimension, m	LB	UB
L	2	25
W_a	0.5	9.3
f	0.2	3
D_i	0.01	0.04
Dg_i	0.11	0.15

Table 3 Variables range on the parametric analysis

Figure 11 shows the variation of the PVLCES and the total integrated heat with the length, L. It can be observed that the PVLCES becomes negative for some values of L. On the other hand, as the length increases, the total integrated heat increases in a linear manner.

The effect of the variation of the aperture, W_a, is depicted in Figure 12. It can be observed that there is an optimum where both the PVLCES and the total integrated heat are maximised.

ISSN 2523-2881

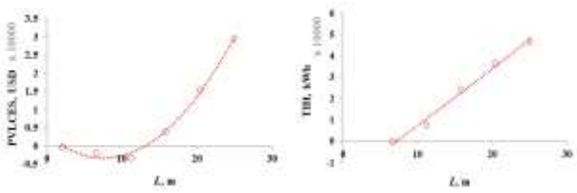

Figure 11 Effect of length, **L**, on the PVLCES and total integrated heat for a typical day in summer

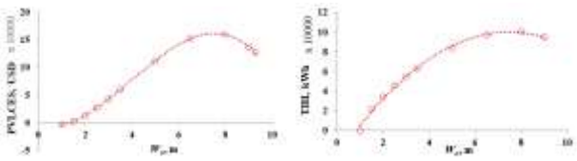

Figure 12 Effect of the aperture on the PVLCES and total integrated heat for a typical day in summer

The effect of the focal length, ***f***, is shown in Figure 13. The profiles indicate that after certain value of ***f***, the increment of this variable has minimal effect of PVLCES and total integrated heat.

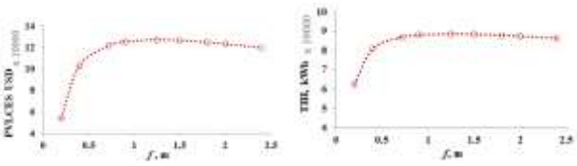

Figure 13 Effect of the focal length on PVLCES and total integrated heat for a typical day in summer

The variation of the inner diameter of the receiver tube, D_i, and the glass cover, Dg_i, is displayed in Figures 14 and 15 respectively.

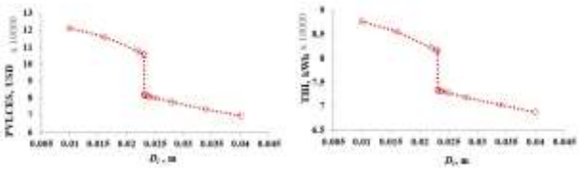

Figure 14 Effect of the inner diameter of the receiver tube, D_i, on the PVLCES and the total integrated heat for a typical day in summer

For the inner diameter of the receiver tube, it is observed that at certain value the PVLCES and total integrated heat drop drastically ($D_i \approx 0.023$ m). On the other hand, the variation of the inner diameter of the glass cover does not affect significantly any of the parameters.

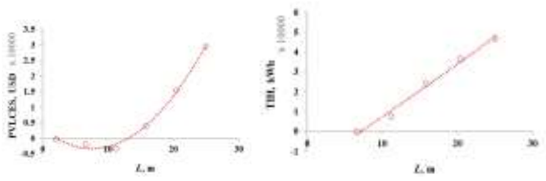

Figure 15 Effect of the inner diameter of the glass cover, Dg_i on the PVLCES and total integrated heat for a typical day in summer

Finally, Figure 16 shows the effect of the type of working fluid on the parameters.

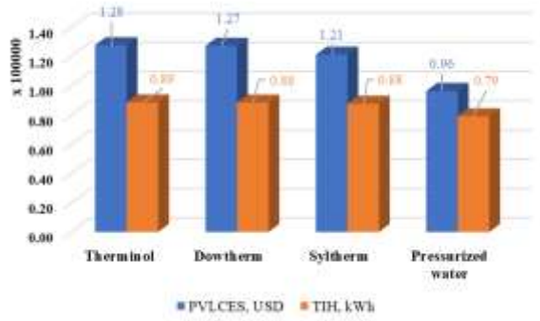

Figure 16 Effect of the type of working fluid on PVLCES and total integrated heat for a typical day in summer

In this study, the working fluid for which the highest performance is obtained is Therminol followed by Dowtherm. The performance with the different thermal oils is similar while the use of pressurised water renders the lowest performance.

Conclusions

Form the results obtained, the following conclusions are drawn:

1. Due to the high non-linearity of the thermal model, the sequential solution approach ensures that the correct solution is found.

2. The thermal model was validated against experimental data and statistical indicators reported by other models in the open literature. This ensures the reliability of the new model.

3. The present value of the life cycle energy savings (PVLCES) is a useful parameter that allows to determine the economic feasibility of the installation of a solar thermal plant.

ISSN 2523-2881

4. From the parametric analysis it can be concluded that the diameter of the cover glass is the design variable has the minimal impact on the economic performance and total heat recovered. On the contrary, the length and PTC width are the variables that bear the strongest influence.

5. The inner diameter of the receiver tube favours the thermal efficiency. At lower dimensions the Re number increases and the heat transfer capacity as well. The analysis of this variable exhibits an abrupt discontinuity which increases the complexity of the solution.

6. Amidst the working fluids, the thermal oils have similar high performance but are much higher than that obtained with pressurised water.

7. The new thermal model is suitable to be used in optimisation and control studies due to its transient nature.

8. Future work underway is the design optimisation of PTC for industrial applications. A metaheuristic algorithm is proposed given the high nonlinearity of the system and the apparent discontinuity of the performance with the inner diameter of the receiver tube.

Acknowledgments

Juan Ramón Lizárraga Morazán is grateful to CONAHCyT and the Department of Chemical Engineering of the Division of Natural and Exact Sciences of the University of Guanajuato, for the support in the development of this research.

References

[I] Philibert, C. Insight Series. 2017.

[II] Birol, F. World Energy Investment. 2023, 1–183.

[III] Pramanik, S.; Ravikrishna, R. V. A Review of Concentrated Solar Power Hybrid Technologies. Appl Therm Eng 2017, 127, 602–637, doi:10.1016/j.applthermaleng.2017.08.038.

[IV] Awan, A.B. Comparative Analysis of 100 MW Concentrated Solar Power Plant and Photovoltaic Plant. AIP Conf Proc 2019, 2119, doi:10.1063/1.5115363.

[V] Salgado Conrado, L.; Rodriguez-Pulido, A.; Calderón, G. Thermal Performance of Parabolic Trough Solar Collectors. Renewable and Sustainable Energy Reviews 2017, 67, 1345–1359, doi:10.1016/j.rser.2016.09.071.

[VI] Spork-Dur, W. Solar Heat World Wide. 2022, 88; https://www.iea-shc.org/Data/Sites/1/publications/Solar-Heat-Worldwide-2022.pdf. Acceso: 10 julio 2023.

[VII] Xu, L.; Sun, F.; Ma, L.; Li, X.; Lei, D.; Yuan, G.; Zhu, H.; Zhang, Q.; Xu, E.; Wang, Z. Analysis of Optical and Thermal Factors' Effects on the Transient Performance of Parabolic Trough Solar Collectors. Solar Energy 2019, 179, 195–209, doi: 10.1016/j.solener.2018.12.070.

[VIII] Adib, R.; Zervos, A. Renewables 2023 Global Status Report; 2023; https://www.ren21.net/wp-content/uploads/2019/05/GSR2023_Demand_Modules.pdf. Acceso: 9 julio 2023.

[IX] Kalogirou, S. Solar Energy Engineering. [Electronic Resource] : Processes and Systems. 2009.

[X] Zima, W.; Cebula, A.; Cisek, P. Mathematical Model of a Sun-Tracked Parabolic Trough Collector and Its Verification. Energies (Basel) 2020, 13, doi:10.3390/en13164168.

[XI] Behar, O.; Khellaf, A.; Mohammedi, K. A Novel Parabolic Trough Solar Collector Model - Validation with Experimental Data and Comparison to Engineering Equation Solver (EES). Energy Convers Manag 2015, 106, 268–281, doi: 10.1016/j.enconman.2015.09.045.

[XII] Ferchichi, S.; Kessentini, H.; Morales-Ruiz, S.; Rigola, J.; Bouden, C.; Oliva, A. Thermal and Fluid Dynamic Analysis of Direct Steam Generation Parabolic Trough Collectors. Energy Convers Manag 2019, 196, 467–483, doi:10.1016/j.enconman.2019.05.107.

[XIII] Mouaky, A.; Alami Merrouni, A.; Laadel, N.E.; Bennouna, E.G. Simulation and Experimental Validation of a Parabolic Trough Plant for Solar Thermal Applications under the Semi-Arid Climate Conditions. Solar Energy 2019, 194, 969–985, doi:10.1016/j.solener.2019.11.040.

[XIV] Krishna, Y.; Faizal, M.; Saidur, R.; Manihalla, P.P.; Karinka, S. Performance Analysis of Parabolic Trough Collector Using TRNSYS®-A Case Study in Indian Coastal Region. J Phys Conf Ser 2021, 1921, doi:10.1088/1742-6596/1921/1/012063.

[XV] Chapra, S.C. Applied Numerical Methods With Matlab® For Engineers And Scientists; McGrawHill Education, Ed.; 4th ed.; New York, 2018.

[XVI] ECMWF Copernicus, Atmosphere Monitoring Service Available online: https://atmosphere.copernicus.eu/, acceso: 2 junio 2023.

[XVII] Caballero-Esparza, M.; Lizárraga-Morazán, J.R.; Picón-Núñez, M. Economic Analysis for the Selection of Low Temperature Solar Thermal Utility Systems. Appl Therm Eng 2022, 215, 118913, doi: 10.1016/j.applthermaleng.2022.118913.

[XVIII] Dudley, E.; Kolb, J.; Mahoney, A.; Mancini, T.; M, S.; Kearney, D. Test Results: SEGS LS-2 Solar Collector. Sandia National Laboratory. Report: SAND94- 1884. 1994, 140.

[XIX] Yilmaz, I.H.; Söylemez, M.S. Thermo-Mathematical Modeling of Parabolic Trough Collector. Energy Convers Manag 2014, 88, 768–784, doi: 10.1016/J.ENCONMAN.2014.09.031.

[XX] Padilla, R.V.; Demirkaya, G.; Goswami, D.Y.; Stefanakos, E.; Rahman, M.M. Heat Transfer Analysis of Parabolic Trough Solar Receiver. Appl Energy 2011, 88, 5097–5110, doi: 10.1016/J.APENERGY.2011.07.012.

[XXI]Forristall, R. Heat Transfer Analysis and Modeling of a Parabolic Trough Solar Receiver Implemented in Engineering Equation Solver; Golden, CO (United States), 2003.

[XXII] García-Valladares, O.; Velázquez, N. Numerical Simulation of Parabolic Trough Solar Collector: Improvement Using Counter Flow Concentric Circular Heat Exchangers. Int J Heat Mass Transf 2009, 52, 597–609, doi: 10.1016/J.IJHEATMASSTRANSFER.2008.08.004.

[XXIII] Meyers; R.A. Encyclopedia of Sustainability Science and Technology 2013, 7619–7622.

ISSN 2523-2881